Published in final edited form as:
Radiat Prot Dosimetry. 2006 ; 122(1-4): 275–281. doi:10.1093/rpd/ncl433.

A MODEL FOR THE INDUCTION OF CHROMOSOME ABERRATIONS THROUGH DIRECT AND BYSTANDER MECHANISMS

H. Schöllnberger[1,*], **R. E. J. Mitchel**[2], **D. J. Crawford-Brown**[3], and **W. Hofmann**[1]

[1]Department of Material Sciences, University of Salzburg, Hellbrunnerstrasse 34, A-5020 Salzburg, Austria

[2]Atomic Energy of Canada Limited, Chalk River Laboratories, Chalk River, Ontario, Canada K0J 1J0

[3]Carolina Environmental Program, University of North Carolina at Chapel Hill, NC 27599-1105, USA

Abstract

A state vector model (SVM) for chromosome aberrations and neoplastic transformation has been adapted to describe detrimental bystander effects. The model describes initiation (formation of translocations) and promotion (clonal expansion and loss of contact inhibition of initiated cells). Additional terms either in the initiation model or in the rate of clonal expansion of initiated cells, describe detrimental bystander effects for chromosome aberrations as reported in the scientific literature. In the present study, the SVM with bystander effects is tested on a suitable dataset. In addition to the simulation of non-linear effects, a classical dataset for neoplastic transformation in C3H 10T1/2 cells after alpha particle irradiation is used to show that the model without bystander features can also describe LNT-like dose responses. A published model for bystander induced neoplastic transformation was adapted for chromosome aberration induction and used to compare the results obtained with the different models.

INTRODUCTION

The state vector model (SVM) is a multistage model for initiation and promotion. Some of the most important biological features associated with these stages of carcinogenesis are formulated mathematically in terms of coupled differential equations to yield either the number of chromosome aberrations per cell or the neoplastic transformation frequency per surviving cell (TF/SC)(1-5). Recent studies with this model(4) focused on the description of protective effects of low doses of low-linear energy transfer (LET) radiation as discovered in recent years(6-8).

Detrimental and protective bystander effects are of great interest because of their importance at low doses(9-12). Different pathways have been investigated to determine how radiation can damage cells that were not directly hit. Radiation may also initiate at the time of exposure by targeted or untargeted effects. Initiation may be post-exposure due to untargeted effects and bystander effects may promote pre-existing initiated cells(13,14).

*Corresponding author: helmut.schoellnberger@sbg.ac.at.

Europe PMC Funders Author Manuscripts

The current study was performed to implement detrimental bystander effects into a multistage model that describes initiation, via the formation of chromosome translocations, and promotion via loss of contact inhibition and a selective growth advantage (enhanced cell proliferation) of a fraction of the initiated cells. Others have presented models for bystander effects for neoplastic transformation, cell killing and cancer(15-23). The model presented here allows for a dose dependent description of bystander effects for chromosome aberrations with the bystander effect being the largest at small doses. The model with bystander effects is tested on a suitable dataset that shows detrimental bystander effects for chromosome aberrations(24). The model without bystander effects is fit to a set of data by Miller *et al.*(25) that shows an LNT-like dose–response curve for neoplastic transformation. A published bystander model for neoplastic transformation, the *B*a*D* model(15), is adapted for chromosome aberrations and applied to the data by Nagasawa and Little(24) to allow for a comparison of the two models.

MATERIALS AND METHODS

The models

The model equations of the SVM (Figure 1) without bystander effects are as follows:

$$\frac{dN_0}{dt} = (k_m - k_{01s} - k_{01ns} - k_d) N_0 + (k_{rs} + 2 \times k_m) N_{1s} + (k_{rns} + 2 \times k_m) N_{1ns} + (k_{rs} + k_{rns} + 2 \times k_m) N_2. \quad (1)$$

$$\frac{dN_{1s}}{dt} = k_{01s} N_0 - (k_{01ns} + k_{rs} + k_m + k_d) N_{1s}. \quad (2)$$

$$\frac{dN_{1ns}}{dt} = k_{01ns} N_0 - (k_{01s} + k_{rns} + k_m + k_d) N_{1ns}. \quad (3)$$

$$\frac{dN_2}{dt} = k_{01ns} N_{1s} + k_{01s} N_{1ns} - (k_{rs} + k_{rns} + k_{23} + k_m + k_d) N_2. \quad (4)$$

$$\frac{dN_3}{dt} = k_{23} N_2 + (k_{m3} - k_{34} - k_d) / N_3. \quad (5)$$

$$\frac{dN_4}{dt} = k_{34} N_3 + \left(F \times k_{mp} + (1 - F) \times k_m - k_d\right) N_4. \quad (6)$$

Here, $N_i(t)$ is the number of cells in state i at time t. Normal cells (state 0) can divide with mitotic rate k_m (cell divisions per day), die with rate k_d ($k_d = k_{db} + k_{dr} \times$DR) or acquire a double strand break (DSB) in transcriptionally active DNA and develop into state 1s cells with rate k_{01s} ($k_{01s} = k_{01sb} + k_{01sr} \times$DR). The subscript b denotes background, subscript r denotes radiation-induced. The dose rate of the irradiation is denoted as DR. When normal cells receive a DSB in transcriptionally inactive DNA, they develop into state 1*ns* cells with rate k_{01ns} ($k_{01ns} = k_{01nsb} + k_{01nsr} \times$DR). These DSBs can undergo repair with rate k_{rns}. The DSBs in state 1*s* cells can be repaired with rate k_{rs}. State 2 cells contain both DSBs. In the SVM, DSB repair with a rate equal to the mitotic rate k_m is allowed for cells in states 1*s*, 1*ns* and 2 (Figure 1). It is emphasised that despite its relation to k_m this repair does not happen during mitosis. All three repair opportunities (k_{rs}, k_{rns} and the cell cycle associated repair)

represent homologous recombination (HR) and non-homologous end-joining (NHEJ). Each cell cycle associated repair event produces two undamaged cells in state 0 (refer to Equation 1). DSBs in state 2 cells can also be repaired with rate $k_{rs}+k_{rns}$. When a suitable interaction [rate $k_{23} = k_{23r}\times(\mathrm{DR}_b+\mathrm{DR})$] occurs between the specific and the non-specific DSB, chromosome aberrations are produced with rate $k_{34} = P_4\times k_m$. It was assumed that $\mathrm{DR}_b = 1$ mGy y^{-1}. In the SVM, chromosome aberrations are characteristic for initiated cells (state 4). This severe damage can no longer be repaired because it was fixed (made permanent) when state 3 cells underwent mitosis with rate $k_{m3} = (1-P_4)\times k_m$. Cells in states 1*s*, 1*ns*, 2, 3 and 4 can die with rate k_d. A fraction, F, of the initiated cells has a growth advantage and divides with an enhanced mitotic rate $k_{mp}= k_{mmult}\times k_m$. In this subpopulation, intercellular communication has been disrupted. The other fraction, $(1-F)$, of initiated cells divides at rate k_m. The fraction F is calculated with a binomial distribution as the probability that an initiated cell is surrounded by 4, 5 or 6 dead cells.

To describe detrimental bystander effects, a dose dependent term $k_{01b\_by}\times\exp(-\lambda_{1by}\times\mathrm{D})$ was added to the rates k_{01s} and k_{01ns}. This reflects the above mentioned possibility that initiation may be postexposure due to untargeted effects. Alternatively, a dose and dose rate dependent term $k_{01r\_by}\times\mathrm{DR}\times\exp(-\lambda_{2by}\times D)$ was added to rate k_{01ns} [but not to k_{01s} because in the SVM $k_{01sr} = 0$(1)]. This reflects the possibility that radiation may initiate cells at the time of exposure by untargeted effects. A third possibility to account for bystander effects is to multiply k_m in Equation 6 with $[1+k_{m\_by}\times\exp(-\lambda_{3by}\times D)]$. This accounts for the finding that bystander effects may promote pre-existing initiated cells.

According to the *BaD* model by Brenner *et al.*(15) for broad beam irradiation, the predicted TF/SC is given as

$$\mathrm{TF/SC}=\nu q\langle N\rangle+\sigma\left[1-\mathrm{e}^{-k\langle N\rangle}\right]\mathrm{e}^{-q\langle N\rangle}, \quad (7)$$

where ν is the slope of the linear dose response relationship, q is the probability of surviving a single alpha particle traversal, $\langle N\rangle$ is the mean number of poisson distributed alpha particle nuclear traversals and σ is the fraction of cells that are hypersensitive to transformation by the bystander signal. The number of unirradiated neighbour cells that receive a bystander signal from hit cells is denoted as k(15).

Equation 7 can be adapted for direct and bystander-induced chromosome aberration formation and becomes

$$\mathrm{CA/SC}=\nu q\langle N\rangle+\sigma\left[1-\mathrm{e}^{-k\langle N\rangle}\right]\mathrm{e}^{-q\langle N\rangle}, \quad (8)$$

where CA/SC is the total number of chromosome aberrations per surviving cell and σ is the fraction of cells that are hypersensitive to chromosome aberration formation by the bystander signal. The definition of the other parameters in Equation 8 remains the same as given for Equation 7. When $\langle N\rangle$ is large (i.e. at high doses), Equation 7 reduces to a linear response TF/SC = $\nu q\langle N\rangle$ or, equivalently, TF/SC = αD(15). Here, D is the absorbed dose. From $\nu q\langle N\rangle \equiv \alpha D$ it follows that $q\langle N\rangle = \alpha D/n$. With the definition $\beta \equiv \alpha/\nu$, we get $q\langle N\rangle = \nu D$. Since $\langle N\rangle$ and D are directly proportional(15), we can write $\langle N\rangle = \gamma D$ where γ is a proportionality constant. Therefore,

$$\mathrm{CA/SC}=\alpha D+\sigma\left[1-\mathrm{e}^{-\delta D}\right]\mathrm{e}^{-\beta D} \quad (9)$$

Europe PMC Funders Author Manuscripts

with $\delta \equiv k\gamma$.

The data

The first dataset is from Nagasawa and Little(24). These data show a detrimental bystander effect in wild type Chinese hamster ovary (CHO) and xrs-5 cells for chromosome aberrations after broad beam irradiation with 3.7 MeV alpha particles of 112 keV μm^{-1} at a dose rate of 0.099 Gy min^{-1}. The cell line xrs-5 is an X-ray sensitive mutant of CHO cells and is deficient in NHEJ[defect in Ku80, a component of the NHEJ pathway(26)]. The mean doubling time for CHO and xrs-5 cells is 12 h ($k_m = 2\ d^{-1}$) and 13 h ($k_m = 1.85\ d^{-1}$), respectively(24). The duration of the sham irradiation was 30 min (H. Nagasawa, personal communication). Analysis of chromosome aberrations was at 19 h after the irradiation (H. Nagasawa, personal communication). As Nagasawa and Little(24) do not present survival fractions, the survival data for alpha particles given in Nagasawa and Little(27) were used to estimate k_{dr}. xrs-5 cells were significantly more sensitive to the induction of aberrations by low doses of alpha radiation (Figure 2).

The other dataset was taken from Miller *et al.*(25) with additional information on irradiation times kindly provided by S. Marino. These data refer to acute irradiation of C3H 10T1/2 cells with alpha particles of 150 keV μm^{-1}. The biological endpoint is neoplastic transformation. The data are given in Table 1. The irradiation times refer to one cell and not to a whole flask (S. Marino, personal communication). Both datasets for 150 keV μm^{-1} of Miller *et al.*(25) (depicted in Figure 3) were fit jointly.

Optimisation procedures

A grid search optimisation procedure developed earlier (Lauren Fleishman, personal communication) was adapted. For n free parameters, the summed relative errors were calculated for an n-dimensional space of parameter combinations and a minimum value was found in an n-dimensional matrix of relative errors. The parameter value combination that corresponded to this minimum summed relative error value was chosen as the optimal unknown parameter combination. For some of the fits, however, the least square based error was applied because it yielded a better fit than the relative error.

RESULTS

At first, the survival fractions of both datasets were fit with the radiation-dependent survival term of the SVM, $\exp(-k_{dr}D)$, to get an estimate for k_{dr}. For the Nagasawa and Little data(24) $k_{dr} = 2.11\ Gy^{-1}$. For the Miller *et al.* data(25) $k_{dr} = 2.13\ Gy^{-1}$ (fits not shown). For the simulation of the data of Nagasawa and Little(24), the model Equations 1-6 were solved numerically with Matlab© for the exposure time (ET) and for the 19 h growth period. The data show the total number of chromosome aberrations per (surviving) cell which in the SVM corresponds to $N_4(t)/[N_0(t)+N_{1s}(t)+N_{1ns}(t)+N_2(t)+N_3(t)+N_4(t)]$ with t = ET+19 h. This expression was multiplied with a suitable proportionality constant (10^5). This reflects the fact that only a fraction of the measured chromosome aberrations will initiate a cell(2). As the formation of chromosome aberrations does not involve promotion, $F = 0$ was applied.

For the fit of the wild-type CHO cells the model without bystander effects was at first fit to the control and the high dose data points at 1 and 2 Gy to get estimates for k_{01sb}, k_{01nsb} and k_{01nsr} (fit1, Table 2). The model was then fit to the whole dataset with the different options to account for the bystander effect as outlined above (using the best estimated values for k_{01sb}, k_{01nsb}, k_{01nsr} as fixed input). At first, the term $k_{01b\_by}\times\exp(-\lambda_{1by}\times D)$ was added to k_{01s} and k_{01ns}. Figure 2A gives the best fit to the data and also shows the separate contributions of the direct (fit 1) and the bystander effects. The best estimates of the model

Europe PMC Funders Author Manuscripts

fit to the full dataset are given in Table 2 (fit2, denoted as 'total' in the legend of Figure 2A). The bystander effect is switched-off at '0' dose (i.e. $k_{01b\_by} = 0$ at dose '0'). In an alternative approach the term $k_{01r\_by} \times \mathrm{DR} \times \exp(-\lambda_{2by} \times D)$ was added to k_{01ns}. However, it was not possible to fit the data with this approach because this term is only ≠0 during the rather short ETs and therefore cannot adequately account for the bystander effect. A fit (not shown) equally good to the one depicted in Figure 2A was achieved by multiplying k_m in Equation 6 with the term $1+k_{m\_by} \times \exp(-\lambda_{3by} \times D)$.

For the fit of the xrs-5 data an analogous procedure was used. To account for the deficiency of NHEJ in this cell line, k_{rs}, k_{rns} and k_m of the cell cycle associated repair were divided by a reduction factor, λ_{red}. The best fit to the xrs-5 data is depicted in Figure 2B. The best estimates are provided in Table 2 (fit3, fit4). The other two approaches to account for the bystander effect yielded analogous results (not shown) as in the fits of the wild-type data.

The adapted *BaD* model (Equation 9) was successfully fit to the data by Nagasawa and Little(24). At first, the linear part, αD, was fit to control and high dose data for CHO cells yielding a best estimate for α of 1.02 Gy^{-1}. Then the whole Equation 9 was fit to the full dataset (Figure 2C) with $\alpha \equiv 1.02\ \mathrm{Gy}^{-1}$. The best estimates were $\beta = 1.35\ \mathrm{Gy}^{-1}$, $\sigma = 0.44$ and $\delta = 11.11\ \mathrm{Gy}^{-1}$. The xrs-5 cells were fit analogously (Figure 2D). Figures 2C and D also delineate the separate contributions of direct (αD) and bystander effects ($\sigma[1-e^{-\delta D}]e^{-\beta D}$).

The model without bystander effects was also tested on a dataset for C3H 10T1/2 cells(25). The mean doubling time of the C3H 10T1/2 cells used by Miller's group is ~20 h(28). Therefore, $k_m = 1.2\ \mathrm{d}^{-1}$. The duration of the exponential growth was calculated to be 6.75 d. The Miller *et al.* experiment lasted for 42 d(25). The model equations were solved accordingly. The values of the three free parameters were estimated from 12 data points. The best estimates are given in Table 2 (fit5). Initial model fits revealed that k_{mmult} was ~1. Therefore, $k_{mmult} \equiv 1$ was used. Figure 3 shows the best fit to the data. For all SVM fits, the values of the other parameters (k_{db}, k_{rs}, k_{rns}, k_{23r} and P_4) were taken from earlier studies(1,5).

DISCUSSION AND CONCLUSIONS

The first model for detrimental bystander effects was the *BaD* model for neoplastic transformation by Brenner *et al.*(15). However, to the best of our knowledge this is the first time a bystander model for chromosome aberrations has been presented. The results show that the *BaD* model from Brenner *et al.*(15), adapted for chromosome aberrations, fits the data of Nagasawa and Little(24) well (Figure 2C and D). Both approaches (SVM and adapted *BaD* model) have a limited number of free parameters. The SVM is based on biological mechanisms relevant for initiation and promotion. The *BaD* model does not include such mechanisms but contains a simple model for bystander-induced signalling. The latter is currently not explicitly included in the SVM. The mathematical form of the adapted *BaD* model for broad beam irradiation (Equation 9) is similar to the initiation rates, k_{01s} and k_{01ns}, of the SVM. Both contain direct terms and a bystander term that decreases exponentially with increasing dose.

The data depicted in Figure 3 have been successfully analysed before with an earlier version of the SVM(5). The new version of the SVM is, however, easier to fit than the earlier version which required separate fitting approaches for the initiation and the promotion models. The role of HR and NHEJ in the bystander effect for chromosome aberrations has recently been studied(29,30). These papers also provide datasets on bystander induced chromosome aberrations in wild type and repair deficient mammalian cell lines. For the current study, it was decided to use the data from Nagasawa *et al.*(24) as they provide more

data points than the other more recent publications. The study shows that the SVM can be used to describe non-linear features in dose responses, such as detrimental bystander effects, but also LNT-shaped curves.

Acknowledgments

We gratefully acknowledge the support of Steve Marino and Dr R. C. Miller (both: Columbia University) in providing irradiation times and for related fruitful discussions. We thank Dr Robert D. Stewart, Purdue University, for fruitful discussions and for critically reading the manuscript. We also acknowledge fruitful discussions with Dr Hatim Fakir, University of Salzburg. This work was supported by the RISC-RAD Project (EC Contract Number FI6RCT-2003-508842), by a Marie Curie European Reintegration Grant within the 6th European Community Framework Program (EC Contract No MERG-CT-2004-006610) and by the Austrian Science FundFWF (project P18055-N02). We also acknowledge support from Atomic Energy of Canada Limited. Funding to pay the Open Access publication charges for this article was provided by the Austrian Science Fund FWF.

REFERENCES

1. Crawford-Brown DJ, Hofmann W. A generalized state-vector model for radiation-induced cellular transformation. Int. J. Radiat. Biol. 1990; 57(2):407–423. [PubMed: 1968504]
2. Schöllnberger H, Kotecki MR, Crawford-Brown DJ, Hofmann W, Eckl PM. Adaptive response and dose-response plateaus for initiation in a state-vector model of carcinogenesis. Int. J. Radiat. Biol. 1999; 75(3):351–364. [PubMed: 10203185]
3. Schöllnberger H, Mitchel REJ, Crawford-Brown DJ, Hofmann W. Nonlinear dose-response relationships and inducible cellular defence mechanisms. J. Radiol. Prot. 2002; 22(3A):A21–A25. [PubMed: 12400942]
4. Schöllnberger H, Mitchel REJ, Azzam EI, Crawford-Brown DJ, Hofmann W. Explanation of protective effects of low doses of γ-radiation with a mechanistic radiobiological model. Int. J. Radiat. Biol. 2002; 78(12):1159–1173. [PubMed: 12556343]
5. Mebust MR, Crawford-Brown DJ, Hofmann W, Schöllnberger H. Testing extrapolation of a biologically-based exposure-response model from in vitro to in vivo to human epidemiological conditions. Reg. Toxicol. Pharmacol. 2002; 35(1):72–79.
6. Azzam EI, de Toledo SM, Raaphorst GP, Mitchel REJ. Low-dose ionizing radiation decreases the frequency of neoplastic transformation to a level below the spontaneous rate in C3H 10T1/2 cells. Radiat. Res. 1996; 146(4):369–373. [PubMed: 8927708]
7. Redpath LJ, Antoniono RJ. Induction of an adaptive response against spontaneous neoplastic transformation in vitro by low-dose gamma radiation. Radiat. Res. 1998; 149(5):517–520. [PubMed: 9588363]
8. Redpath JL, Liang D, Taylor TH, Christie C, Elmore E. The shape of the dose response curve for radiation-induced neoplastic transformation in vitro: evidence for an adaptive response against neoplastic transformation at low doses of low-LET radiation. Radiat. Res. 2001; 156(6):700–707. [PubMed: 11741493]
9. Morgan WF. Non-targeted and delayed effects of exposure to ionizing radiation: I. Radiation-induced genomic instability and bystander effects in vitro. Radiat. Res. 2003; 159(5):567–580. [PubMed: 12710868]
10. Morgan WF. Non-targeted and delayed effects of exposure to ionizing radiation: II. Radiation-induced genomic instability and bystander effects in vivo, clastogenic factors and transgenerational effects. Radiat. Res. 2003; 159(5):581–596. [PubMed: 12710869]
11. Iyer R, Lehnert BE. Alpha-particle-induced increases in the radioresistance of normal human bystander cells. Radiat. Res. 2002; 157(1):3–7. [PubMed: 11754635]
12. Belyakov OV, Folkard M, Mothersill C, Prise KM, Michael BD. Bystander-induced apoptosis and premature differentiation in primary urothelial explants after charged particle microbeam irradiation. Radiat. Prot. Dosim. 2002; 99(1–4):249–251.
13. Lorimore SA, Wright EG. Radiation-induced genomic instability and bystander effects: related inflammatory-type responses to radiation-induced stress and injury? A review. Int. J. Radiat. Biol. 2003; 79(1):15–25. [PubMed: 12556327]

14. Coates PJ, Lorimore SA, Wright EG. Damaging and protective cell signalling in the untargeted effects of ionizing radiation. Mutat. Res. 2004; 568(1):5–20. [PubMed: 15530535]
15. Brenner DJ, Little JB, Sachs RK. The bystander effect in radiation oncogenesis: II. A quantitative model. Radiat. Res. 2001; 155(3):402–408. [PubMed: 11182790]
16. Stewart RD, Ratnayake RK, Jennings K. Microdosimetric model for the induction of cell killing through medium-borne signals. Radiat. Res. 2006; 165(4):460–469. [PubMed: 16579659]
17. Little MP, Wakeford R. The bystander effect in C3H 10T1/2 cells and radon-induced lung cancer. Radiat. Res. 2001; 156(6):695–699. [PubMed: 11741492]
18. Brenner DJ, Sachs RK. Do low dose-rate bystander effects influence domestic radon risks? Int. J. Radiat. Biol. 2002; 78(7):593–604. [PubMed: 12079538]
19. Khvostunov IK, Nikjoo H. Computer modelling of radiation-induced bystander effect. J. Radiol. Prot. 2002; 22(3A):A33–A37. [PubMed: 12400944]
20. Nikjoo H, Khvostunov IK. Biophysical model of the radiation-induced bystander effect. Int. J. Radiat. Biol. 2003; 79(1):43–52. [PubMed: 12556330]
21. Nikjoo H, Khvostunov IK. A theoretical approach to the role and critical issues associated with bystander effect in risk estimation. Hum. Exp. Toxicol. 2004; 23(2):81–86. [PubMed: 15070065]
22. Little MP, Filipe JA, Prise KM, Folkard M, Belyakov OV. A model for radiation-induced bystander effects, with allowance for spatial position and the effects of cell turnover. J. Theor. Biol. 2005; 232(3):329–338. [PubMed: 15572058]
23. Sachs RK, Chan M, Hlatky L, Hahnfeldt P. Modeling intercellular interactions during carcinogenesis. Radiat. Res. 2005; 164(3):324–331. [PubMed: 16137206]
24. Nagasawa H, Little JB. Bystander effect for chromosomal aberrations induced in wild-type and repair deficient CHO cells by low fluences of alpha particles. Mutat. Res. 2002; 508(1–2):121–129. [PubMed: 12379467]
25. Miller RC, Marino SA, Brenner DJ, Martin SG, Richards M, Randers-Pehrson G, Hall EJ. The biological effectiveness of radon-progeny alpha particles. II. Oncogenic transformation as a function of linear energy transfer. Radiat. Res. 1995; 142(1):54–60. [PubMed: 7899559]
26. Nagasawa H, Huo L, Little JB. Increased bystander mutagenic effect in DNA double-strand break repair-deficient mammalian cells. Int. J. Radiat. Biol. 2003; 79(1):35–41. [PubMed: 12556329]
27. Nagasawa H, Little JB. Unexpected sensitivity to the induction of mutations by very low doses of alpha-particle radiation: evidence for a bystander effect. Radiat. Res. 1999; 152(5):552–557. [PubMed: 10521933]
28. Miller RC, Geard CR, Martin SG, Marino SA, Hall EJ. Neutron-induced cell cycle-dependent oncogenic transformation of C3H 10T1/2 cells. Radiat. Res. 1995; 142(3):270–275. [PubMed: 7761576]
29. Little JB, Nagasawa H, Li GC, Chen DJ. Involvement of the nonhomologous end joining DNA repair pathway in the bystander effect for chromosomal aberrations. Radiat. Res. 2003; 159(2): 262–267. [PubMed: 12537532]
30. Nagasawa H, Peng Y, Wilson PF, Lio YC, Chen DJ, Bedford JS, Little JB. Role of homologous recombination in the alpha-particle-induced bystander effect for sister chromatid exchanges and chromosomal aberrations. Radiat. Res. 2005; 164(2):141–147. [PubMed: 16038585]

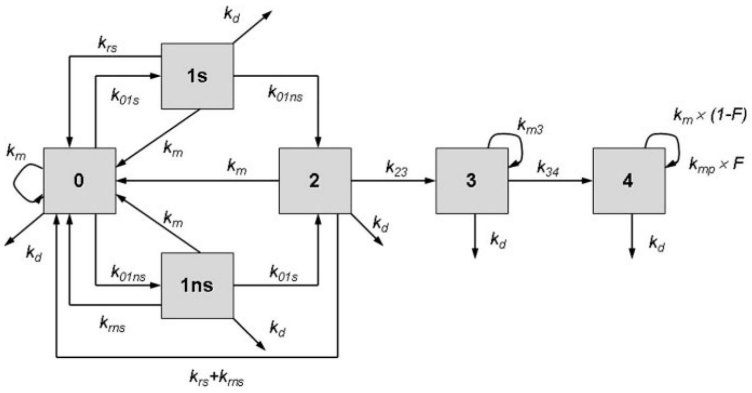

Figure 1.
Pictorial representation of the SVM.

Europe PMC Funders Author Manuscripts

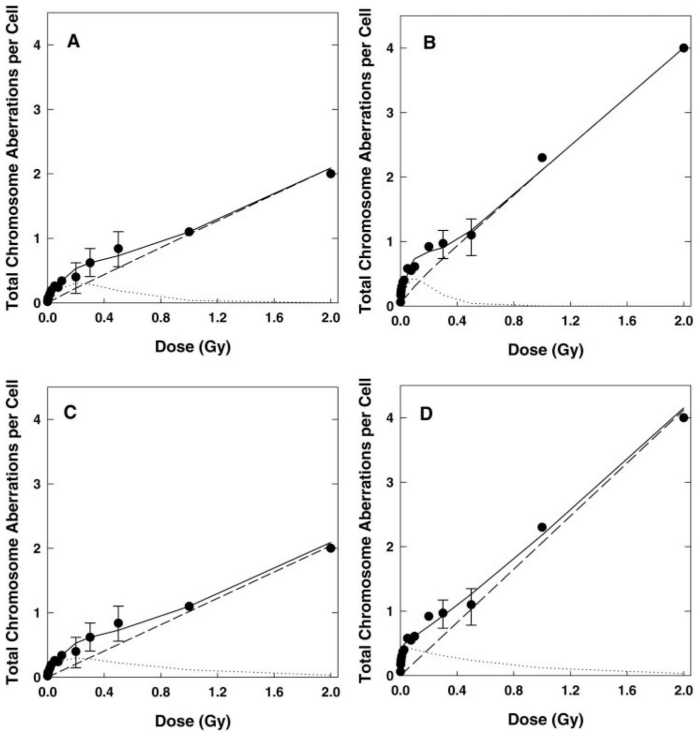

Figure 2.

Total number of chromosome aberrations per cell as a function of the mean dose of alpha radiation. (A) Data for wild-type CHO cells and SVM fit showing the three different contributions (dashed line: direct; dotted line: bystander; full line: total); (B) data for xrs-5 cells and SVM fit; (C) data for wild-type CHO cells and BaD model fit (dashed line: direct; dotted line: bystander; full line: total); (D) data for xrs-5 cells and BaD model fit. The data represent mean values±standard deviations(24). For the SVM fits, the contribution of the bystanders was calculated as the difference between the fitted total (direct+bystander) and the direct CA/SC. The different contributions of the BaD model were obtained by fitting the 'direct' term of Equation 9, aD, to the control and high dose data at 1 and 2 Gy, and the whole Equation 9 to the full dataset. The contribution of the bystander effects was calculated by evaluating $\sigma[1-e^{-\delta D}]e^{-\beta D}$ with the best estimates for σ, δ and β for the doses shown in Figure 2C and D.

Europe PMC Funders Author Manuscripts

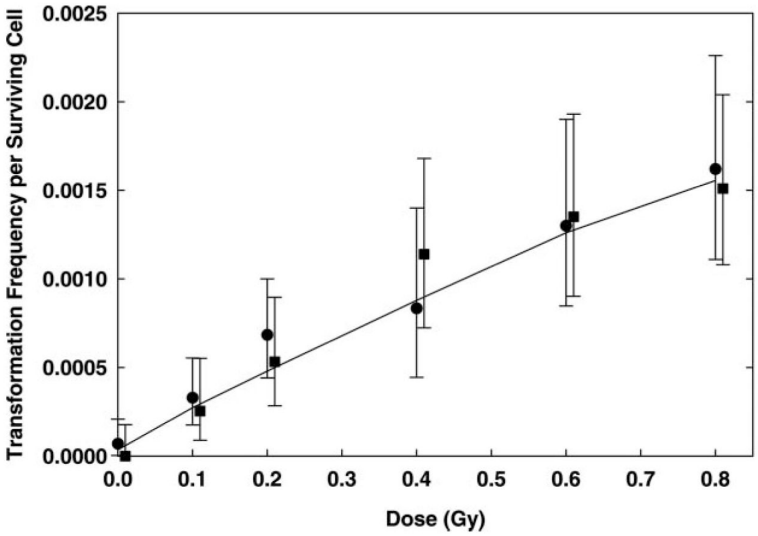

Figure 3.
TF/SC after exposure of C3H 10T1/2 cells to 150 keV μm^{-1} alpha particles(25). Filled circle: first dataset; filled square: second dataset; full line: SVM fit. Here, bystander effects were not included in the model. The error bars represent 95% confidence intervals.

Europe PMC Funders Author Manuscripts

Europe PMC Funders Author Manuscripts

Table 1

Dose, ET, dose rate and TF/SC for alpha particle irradiation (150 keV μm^{-1}) of C3H 10T1/2 cells(25) (S. Marino, personal communication).

Dose (Gy)	ET (s)	Dose rate (Gy s^{-1})	TF/SC
0	0.55	0	6.90×10^{-5}
0.1	0.42	0.237	3.29×10^{-4}
0.2	0.83	0.241	6.84×10^{-4}
0.4	1.68	0.238	8.33×10^{-4}
0.6	2.52	0.238	1.30×10^{-3}
0.8	3.36	0.238	1.62×10^{-3}
0	0.15	0	0
0.1	0.37	0.267	2.54×10^{-4}
0.2	0.75	0.267	5.32×10^{-4}
0.4	1.54	0.259	1.14×10^{-3}
0.6	2.32	0.258	1.35×10^{-3}
0.8	3.07	0.261	1.51×10^{-3}

Europe PMC Funders Author Manuscripts

Table 2

Best estimates and relative errors or least squares-based errors for model fits of the Nagasawa and Little(24) data (fit1 to fit4) and the Miller et al.(25) data for 150 keV μm^{-1} alpha particles (fit5).

Fit1	Fit2	Fit3	Fit4	Fit5
k_{01sb} = 1.9 d^{-1}	k_{01b_by} = 7.1 d^{-1}	λ_{red} = 11.0	k_{01b_by} = 8.1 d^{-1}	k_{01sb} = 11462.8 d^{-1}
k_{01nsb} = 0	λ_{1by} = 4.68 Gy^{-1}		λ_{1by} = 9.6 Gy^{-1}	k_{01nsb} = 0
k_{01nsr} = 25.8 Gy^{-1}				k_{01nsr} = 6497.5 Gy^{-1}
Relative error: 7.776×10^{-2}	Relative error: 4.764	Relative error: 0.318	Least squares-based error: 1.121×10^{-11}	Least squares-based error: 8.179×10^{-8}

In fit1 and fit3 the control and high dose data points at 1 and 2 Gy were fit. The best estimates from fit1 were used as fixed input in fit3. The best estimates from fit1 and fit3 were used as fixed input in fit2 and fit4, respectively, where the model with detrimental bystander features was fit to the full datasets for CHO and xrs-5 cells, respectively. In fit5 $k_{mmult} \equiv 1$